Hydrol. Earth Syst. Sci. Discuss., 8, 7091–7136, 2011
www.hydrol-earth-syst-sci-discuss.net/8/7091/2011/
doi:10.5194/hessd-8-7091-2011

Hydrology and Earth System Sciences Discussions

Inter-comparison of two land-surface schemes applied on different scales and their feedbacks while coupled with a regional climate model

F. Zabel[1], W. Mauser[1], T. Marke[1,2], A. Pfeiffer[3], G. Zängl[3,4], and C. Wastl[3,5]

[1]Department of Geography, Ludwig-Maximilians-Universität, Munich, Germany
[2]Institute of Geography and Regional Sciences, University of Graz, Austria
[3]Institute of Meteorology, University of Munich (LMU), Germany
[4]Deutscher Wetterdienst, Offenbach, Germany
[5]Department of Ecoclimatology, Technical University of Munich (TUM), Germany

Received: 12 July 2011 – Accepted: 18 July 2011 – Published: 20 July 2011

Correspondence to: F. Zabel (f.zabel@iggf.geo.uni-muenchen.de)

Published by Copernicus Publications on behalf of the European Geosciences Union.

Abstract

Feedback effects between the land surface and the atmosphere are an important issue in modelling the climate system. Therefore, in order to take land surface heterogeneity adequately into account, a representation of the land surface in sufficient spatial resolution is necessary. In order to analyze the impact of different land surface models on the atmosphere, we analyzed the differences of two physically based land surface models, which evolved from different disciplinary backgrounds, both fully coupled with the regional climate model MM5, providing the atmospheric drivers. While the NOAH-LSM originally was developed for atmosphere applications, PROMET is primarily used as a hydrological land surface model. Both use different physical approaches and different spatial resolutions of 45 km (NOAH) and 1 km (PROMET) respectively, to represent the land surface processes. The parameterization of soil and plant properties in terms of phenological behaviour and water-stress is treated with a higher level of detail in PROMET. Used with same atmospheric drivers over a four-year period for Central Europe, the model differences have strong impacts on simulated evapotranspiration and soil moisture both spatially and temporally. Regions with high proportion of impervious surfaces show the highest differences in simulated evapotranspiration (up to 30 %). Further, PROMET simulations show lower evapotranspiration rates e.g. in the Po Valley, caused mainly by a higher level of vegetation water stress. In order to study feedback effects, PROMET was then bilaterally coupled with MM5. The feedbacks result in increasing near surface air temperature and decreasing precipitation especially in Southern Europe and are a result of regional self-amplification effects due to decreasing soil moisture and increasing vegetation water stress.

1 Introduction

As much as the land surface is a key element of the climate system, the climatic conditions affect the structure and processes of the land surface (Bounoua et al., 2000). Land surfaces are characterized both by large spatial heterogeneity and by the large diversity and complexity of the physical and biological processes involved. The interactions between the land surface and the atmosphere are based on the exchange of latent and sensible heat, short and longwave radiation as well as momentum (Campbell and Norman, 2000) that affect the atmosphere conditions which in turn feedback on land surface conditions (Bonan, 1995). Land-atmosphere interactions are driven to a large extent by soil moisture and soil temperature, vegetation dynamics and evapotranspiration as well as snow and ice dynamics. A lack of understanding of their complex and spatially heterogeneous interrelation is responsible for one of the key sources of uncertainty in climate simulations (Koster et al., 2004; Koster and Suarez, 1994; Martin, 1998; Orlowsky and Seneviratne, 2010; Pitman, 2003; Zeng et al., 2003).

Land surface schemes (LSSs) used in climate models have undergone large improvements in the past decades. Global climate models (GCMs) have historically concentrated on modelling the largely homogeneous ocean-atmosphere interface at a relatively coarse spatial resolution, paying only little attention to the land surface processes. Primitive land surface models have been applied in climate models that were not able to reproduce observations (Timbal and Henderson-Sellers, 1998).

Regional climate models (RCMs) being forced with exogenous model data on the lateral boundaries of the modelling area, extend the coarse description of atmospheric processes within GCMs towards increased spatial resolution and more process detail, thereby capturing the local structures of each model grid point (Giorgi, 2001; Jacob et al., 2007; Kueppers et al., 2008; Laprise, 2008; Mc Gregor, 1997; Michalakes, 1997; Quintanar et al., 2009; Schär et al., 2004; Stocker, 2004; Zampieri et al., 2011). Nonetheless, the complexity and heterogeneity of land surface processes and the need for a more detailed view of it is a long standing discussion in atmospheric sciences (Henderson-Sellers et al., 1995, 2008; Dickinson, 1995; Dickinson et al., 1991). Therefore, the PILPS-project fundamentally evaluated and improved physically based LSSs for the use in climate models (Dickinson, 1995; Famiglietti and Wood, 1991; Polcher et al., 1998; Wood et al., 1998; Yang et al., 1998; Henderson-Sellers et al., 1996; Timbal and Henderson-Sellers, 1998). There is evidence that more advanced and robust land surface models (LSMs), which increasingly consider the spatial heterogeneity (land-use, soil, elevation) and complexity of land surface biophysical and hydrological processes in the soil-plant-atmosphere continuum on an appropriate scale will reduce the uncertainties in the current modelling of land-atmosphere processes (Essery et al., 2003; Hagemann et al., 2001; Koster et al., 2004; Laprise, 2008; Molod and Salmun, 2002; Seth et al., 1994; Yu, 2000).

Meanwhile, hydrologists have developed empirical, conceptual and more and more physically-based land surface hydrological models (LSHMs) spanning a wide range of complexity. They go beyond reproducing runoff at gauges of small scale catchment areas and now consider in detail the hydrologic land surface processes within the catchment (Bharati et al., 2008; Devonec and Barros, 2002; Garcia-Quijano and Barros, 2005; Kuchment et al., 2006; Kunstmann et al., 2008; Ludwig and Mauser, 2000; Mauser and Bach, 2009; Schulla and Jasper, 1999; Wagner et al., 2009). The physically based models aim at understanding the interactions between the different land surface compartments, namely soil, vegetation, snow and ice in producing the resulting river runoff. They include detailed descriptions of vertical and lateral soil water and energy flows, vegetation dynamics and related flow regulations, snow and ice dynamics as well as energy and mass exchange with the atmosphere, and thereby cover the major land surface processes in the soil-plant-atmosphere continuum. In contrast to LSMs designed for atmosphere applications, the atmosphere is usually considered as exogenous driver only.

At the same time as RCMs become capable of physically downscaling the GCMs outputs to a resolution of 50–10 km, hydrologic land surface models evolve from their original application in small watersheds to large basins. With the improving spatial resolution of the RCMs and the increasing areal coverage of the hydrologic land surface models the scales covered by the two model families tend to converge (Chen et al., 1996; Henderson-Sellers et al., 1995; Yang et al., 1998).

Coupling LSMs with RCMs involves several complex issues such as computational demand as well as the parameterization of the vegetation and soil state (Chen and

HESSD
8, 7091–7136, 2011

Dudhia, 2001a) since these parameters are difficult to specify at a high spatial resolution on continental scales. Current LSMs try to avoid "over-parameterization", thereby keeping their parameterizations simple enough to be sufficient for their physical description of the processes included in the model. However, new research questions such as land use change due to climate change or food production can no longer be answered without taking heterogeneity and feedback effects of the land surface into account on a high level of detail.

In this study, we therefore explore the differences in model physics, parameterization and subsequent fundamental outputs between a classical land surface module for atmospheric models, the NOAH-LSM (Chen and Dudhia, 2001a) and a land surface model from the hydrological model family, PROMET (Mauser and Bach, 2009). While the NOAH-LSM was originally developed for the use in atmosphere applications and often is used within the regional climate model MM5, PROMET represents a hydrological model, originally designed for small- to mesoscale watersheds and spatial resolutions of 100 m to 2 km. The following study covers a region in Central Europe with an extension for 1170 × 1170 km, which is represented by the NOAH-LSM with a spatial resolution of 45 km and by PROMET with a spatial resolution of 1 km.

In a first step, simulated evapotranspiration results of both models were compared while being driven with the same atmospheric inputs, provided by MM5. Here, PROMET was unilaterally coupled with MM5 without returning the land surface energy fluxes to the atmosphere (see Fig. 1). In this case, the lower boundary conditions are provided by the NOAH-LSM. Due to the equal meteorological drivers, the differences between the models related to spatial resolution, model physics and parameterization can be investigated.

Subsequently, the impact of the previously identified differences of latent heat fluxes between both models on the MM5 atmosphere are analyzed by bilaterally coupling PROMET, thus substituting the NOAH-LSM as the lower boundary conditions for MM5 (see Fig. 1).

In order to overcome the different spatial scales between the atmosphere model MM5 (45 km) and PROMET (1 km), a down- and upscaling approach was applied.

Beyond evapotranspiration there are important differences between NOAH-LSM and PROMET such as different snow modules with PROMET altering albedo and shortwave reflection with snow age. In addition, PROMET has a substantially different parameterization of land surface emissivity. All these processes have a strong impact on parameters such as radiation temperature and longwave outgoing radiation. They are not discussed in this paper.

2 Study area

The study area is situated in Central Europe and extends 1170 km north-south by 1170 km east-west including 18 European countries. Plains like the Po and Upper Rhine Valley, uplands like in central Germany and mountainous regions in the Alps, which mark a climatic boundary between the temperate latitudes and the Mediterranean climate, compose a complex landscape. Altitudes are ranging from the Mont Blanc in the French Alps (4810 m) to the Atlantic Ocean in the north-west and the Mediterranean Sea in the south. The area is characterized by intense agriculture especially within the fertile lowlands like the Upper Rhine or the Po Valley and densely populated areas such as the Ruhr region, Berlin, or Milan.

3 Model descriptions

3.1 The atmospheric model MM5

The regional climate model applied in this study is the fifth-generation Mesoscale Model (MM5) (Grell et al., 1994), developed by the Pennsylvania State University (Penn State) and the National Center for Atmospheric Research (NCAR). The widely known model has been used for numerical weather predictions, air quality studies and hydrological studies with grid increment as small as 1 km (Chen and Dudhia, 2001a).

It was modified and adapted to our specific simulation requirements and our specific model domain (Pfeiffer and Zängl, 2009; Zängl, 2002). Here, MM5 is used in climate mode with a single domain having a horizontal spatial resolution of 45 km and an integration internal time step of 135 s. The domain covers most of the European continent and has a size of 79 grid-boxes in west-east and 69 grid-boxes in south-north direction (Pfeiffer and Zängl, 2009). Lateral boundary conditions are provided by 6-hourly ECMWF ERA-40 reanalysis-data (Uppala et al., 2005).

3.2 Land surface schemes

The LSMs applied in this study are the NOAH-LSM and PROMET. Both models describe the pathways of water and energy on the land surface in a physically based manner. The process descriptions at the land surface require meteorological drivers from the atmosphere (Fig. 2) which are provided by MM5. Evapotranspiration which represents the flux of latent heat from the land surface is the main energy flux from the land surface. It is affected by all major properties of and processes on the land surface and therefore is a substantial part of both models. Thus, the main focus of the comparison between the land surface models will be on evapotranspiration.

Evapotranspiration is the sum of plant transpiration via soil, root, leaf and the stomata (E_t) and evaporation from the bare soil (E_{dir}) and evaporation of water intercepted by the canopy or other surfaces (E_i). It is driven by the gradient of vapour pressure between the surface and the surrounding air, passing the laminar boundary layer into the free atmosphere, finally carried away by the turbulent mass transport of wind within the atmospheric boundary layer expressed by the aerodynamic resistance. Thus, modelling the spatially very heterogeneous evapotranspiration is a complex issue which requires taking multiple aspects into account.

$$E = E_{dir} + E_i + E_t \quad (1)$$

HESSD
8, 7091–7136, 2011

The NOAH-LSM is applied at a spatial resolution of 45 km while PROMET is applied with 1 km. Therefore, the models' underlying land-use and soil information as well as the digital elevation model (DEM) vary in spatial heterogeneity. Figure 3 demonstrates this effect by comparing the land use classifications used by NOAH and by PROMET. A detailed description of the land use/cover map used in PROMET is given in (Zabel et al., 2010).

The land cover information has a strong effect on both albedo and partitioning of energy and matter fluxes from the surface to the atmosphere (Ge et al., 2007). Land cover determines the type of vegetation and thereby the seasonal development of plant phenology, canopy structure and leaf area, which in turn, through vegetation height and leaf area index, determines the aerodynamic and evapotranspirative properties of the land surface. The combined vegetation and soil properties determine soil moisture development and the reaction of the land surface to changing fractions of latent and sensible heat fluxes influenced by vegetation water stress.

3.2.1 NOAH-LSM

The NOAH-LSM was originally designed for the use in RCMs and is part of the MM5 modelling system. The NOAH-LSM is an updated version of the OSU-LSM. A complete description of the NOAH and OSU-LSM is given by (Chen and Dudhia, 2001a, b; Mitchell, 2005). The older version of MM5 documented in (Grell et al., 1994) already included a simple land surface model which does not take basic hydrological effects like snow cover into account. The land use had a coarse resolution and soil moisture was defined as a function of land use with seasonal values that cannot change during the simulation or respond to precipitation. Vegetation evapotranspiration and runoff processes were not included (Chen and Dudhia, 2001a).

The goal of the development of the NOAH-LSM was to implement an appropriate LSM for weather prediction and hydrological applications that reflects the major effects of vegetation on the long-term evolution of surface evaporation and soil moisture and to get along with relatively few parameters for short and long-time within

HESSD
8, 7091–7136, 2011

continental-domain applications. The NOAH-LSM is the result of the further developments of LSMs, designed for atmosphere applications over the last years and scientific studies like the PILPS project.

Potential evaporation is calculated within the NOAH-LSM using a Penman-based energy balance approach (Mahrt and Ek, 1984) including a stability-dependent aerodynamic resistance. It includes a 4-Layer soil model and a canopy resistance approach of (Jacquemin and Noilhan, 1990; Noilhan and Planton, 1989). The prognostic variables are the moisture and temperature of the soil layers, water stored on the canopy and snow stored on the ground. Daily surface runoff is computed by the Simple Water Balance (SWB) model (Schaake et al., 1996). The NOAH-LSM computes actual evapotranspiration separately for the following components:

$$E_{\mathrm{dir}} = (1 - \sigma \mathrm{f})\,\beta\,E_{\mathrm{p}} \tag{2}$$

$$E_{\mathrm{i}} = \sigma \mathrm{f}\,E_{\mathrm{p}} \left(\frac{\mathrm{Wc}}{S}\right)^{n} \tag{3}$$

$$E_{\mathrm{t}} = \sigma \mathrm{f}\,E_{\mathrm{p}}\,\mathrm{Bc}\left[1 - \left(\frac{\mathrm{Wc}}{S}\right)^{n}\right] \tag{4}$$

Besides the green vegetation fraction (σ_{f}), the NOAH-LSM is taking the soil water content (β), the intercepted canopy water content (Wc) the maximum canopy capacity (S) as well as a plant coefficient (Bc) as a function of canopy resistance into account (Chen et al., 1996).

The green vegetation fraction (σ_{f}) strongly influences simulation results since it acts as a fundamental weighting coefficient of potential evaporation (E_{p}) within the calculation of all components of evapotranspiration. MM5 uses monthly values of green vegetation fraction (σ_{f}) (also known as F_{cover}) for each grid cell at the model's spatial resolution in order to take seasonal phenological behaviour of vegetation into account. It is defined as a function of NDVI

$$\sigma \mathrm{f} = \frac{\mathrm{NDVI} - \mathrm{NDVI0}}{\mathrm{NDVI}\infty - \mathrm{NDVI0}} \tag{5}$$

Discussion Paper | Discussion Paper | Discussion Paper | Discussion Paper |
HESSD
8, 7091–7136, 2011
Inter-comparison of two land-surface schemes
F. Zabel et al.

where $NDVI_0$ and $NDVI_\infty$ are the lower and upper 5 % of the global NDVI distribution for the whole year and therefore describe the signals from bare soil and not-vegetated areas and dense green vegetation respectively (Chen et al., 1996; Gutman and Ignatov, 1997). Since the $NDVI_\infty$ is likely to reach saturation, this approach tends to overestimate σ_f (Richter and Timmermans, 2009). Uncertainties of NDVI due to soil moisture, soil type and color, dead vegetation and shadow-effects within the plant stand as well as atmospheric effects such as cloud contamination and angular effects of the radiometer field-of-view (FOV) affect satellite-based measurements of the vegetation fraction, making it an unreliable quantity (Bach and Verhoef, 2003; Gutman and Ignatov, 1997; Richter and Timmermans, 2009). Further, the use of the 5th percentile seems arbitrary for global mapping of σ_f since this is only valid for pixels with assumed dense vegetation (Gutman and Ignatov, 1997). The green vegetation fraction concerning this study was gathered by a 5-yr time series of NDVI (Chen et al., 1996; Gutman and Ignatov, 1997) from AVHRR (US Geological Survey (USGS)), with a spatial resolution of 10 min (18.5 km) and global coverage. It was further generally reduced by 30 percent since it proved to be too high for our simulation area and this reduction helped to improve the simulation of summertime near surface temperature substantially (Pfeiffer and Zängl, 2009).

However, it must be pointed out that this approach was introduced by climatologists with the intention of introducing a simple parameter in climate models for worldwide application since it is gathered from satellite data and therefore avoid complex parameterization of individual plants. Also with respect to computational costs, it is a simple and fast approach to implement seasonal behaviour of vegetation. However, it represents a delicate parameter with a large potential of uncertainty due to its impact on evapotranspiration, which results in errors.

Within E_t, the canopy treatment is an important issue. The canopy resistance is formulated as follows in the NOAH-LSM,

$$Rc = \frac{R\text{cmin}}{\text{LAI}\, F_1 F_2 F_3 F_4} \quad (6)$$

where F_4 is the water-stress function with respect to soil moisture while F_1, F_2 and F_3 represent the effects of solar radiation, vapour pressure deficit and air temperature on the canopy resistance. The values of all functions range between 0 and 1; LAI is the leaf area index and R_{cmin} is the minimum canopy resistance which is set to 5000 s m^{-1} for all plants (Jacquemin and Noilhan, 1990; Noilhan and Planton, 1989). The LAI does not change with season and for all land use classes of the NOAH-LSM has a value of 4.0. The temperature-stress function is the same for all plants, the optimum transpiration temperature being parameterized with 298 K (Chen and Dudhia, 2001a). The dynamic function of water-stress (F_4) is a factor for the availability of soil moisture, however neglecting plant specific parameters.

$$F_4 = \sum_{i=1}^{3} \frac{(\Theta i - \Theta w)\mathrm{dz}i}{(\Theta \mathrm{ref} - \Theta w)(\mathrm{dz}1 + \mathrm{dz}2)} \quad (7)$$

It is a function of volumetric soil moisture content (Θ) and the soil specific parameters of field capacity (Θref) and the wilting point (Θw) for the upper three soil layers integrated in the rooted zone (Chen and Dudhia, 2001a), parameterized as percentage values of soil moisture.

3.2.2 PROMET

PROMET was developed for hydrological river catchment studies on the local and regional scale. It is physically based and describes physical processes on the land surface conserving mass and energy with high detail and complexity using several submodules (see Fig. 4) and is used in this study with an hourly temporal and 1 km spatial resolution. An extensive model description can be found in (Mauser and Bach, 2009).

PROMET has already been used in several small and large scale watersheds ranging from a few hundred km^2 to app. 1 mio km^2 and has been extensively validated in different regions in the world (Hank, 2008; Loew, 2008; Loew et al., 2009; Ludwig and Mauser, 2000; Ludwig et al., 2003a, b; Mauser and Bach, 2009; Mauser and Schädlich, 1998; Muerth, 2008; Prasch et al., 2011, 2006; Strasser, 1998; Strasser et al., 2007; Strasser and Mauser, 2001; Weber et al., 2010; Marke et al., 2011a).

Actual evapotranspiration within the vegetation component of PROMET is simulated using the Penman-Monteith equation (Mauser and Schädlich, 1998; Monteith, 1965; Monteith and Unsworth, 2008), closing the energy balance iteratively (Mauser and Bach, 2009). The water pathway via the soil through the roots into the leaf and passing via the stomata into the laminar and finally the turbulent atmosphere, is driven by the potential difference of water vapour between the soil and the atmosphere, assuming that the atmospheric suction is limited by a number of resistances similar to electrical conductivity (Monteith and Unsworth, 2008). The canopy resistance is calculated for individual plant types following an approach by (Baldocchi et al., 1987; Jarvis, 1976). The stomata resistance is a function of radiation (PAR), temperature (F_1), ambient humidity (F_2), CO_2 in the atmosphere (assumed to be constant) and the leaf water potential (F_3) (Jarvis and Morison, 1981).

$$Rc = \frac{R\text{cmin(PAR)}}{F_1 F_2 F_3} \tag{8}$$

PAR is calculated according to the fractions of sunlit and shaded leaf area and the PAR flux densities on the respective leaves (Baldocchi et al., 1987). The relation of temperature, humidity deficit and leaf water potential to the stomata resistance is described with F_1, F_2 and F_3 following (Jarvis, 1976), returning values between 0 and 1. An increase in temperature beyond a plant specific optimum results in an increase of stomata resistance since the plant's stomata will close in order to protect itself against dehydration, which results in a decrease of transpiration. The conductivity is reduced to the minimum stomata conductivity, which is the conductivity of the cuticle.

The inhibition due to water stress is quantified in PROMET in terms of leaf water potential, which depends in a plant-specific way to the soil water potential (ψ_s) within the rooted soil layers.

$$F_3 = ((\Psi\text{s} + R\text{r}) - \Psi 0) * a\Psi + b\Psi \tag{9}$$

HESSD

8, 7091–7136, 2011

The stomatal conductance shows no dependence on leaf water potential below a plant specific threshold (ψ_0) of suction and an approximately linear plant specific decrease beyond (Baldocchi et al., 1987), and takes the resistance of the transition from the soil to the root (R_r) into account (Biscoe et al., 1976). The parameters R_r, ψ_0, a_ψ and b_ψ are parameterized for each plant type in PROMET. The soil water potential is a function of soil type and soil water content following an approach of (Brooks and Corey, 1964).

Overall, PROMET includes a detailed soil and plant parameterization in order to consider the complexity of the physical description of the land surface processes. The parameterization of a wide range of vegetation types in PROMET is taken from literature and remote sensing data (Bach, 1995; Mauser and Bach, 2009). Typical daily change of the plant parameters LAI, albedo, root depth and plant height were taken from the analysis of time series of LANDSAT images in Southern Germany in combination with extensive field measurements on typical plant stands (Mauser and Bach, 2009) thereby taking phenological behaviour of different stands and spatial heterogeneity into account (Zabel et al., 2010). Hence, each plant shows the same phenological behaviour within the study area.

4 Coupling approaches

Since NOAH-LSM is an integral part of MM5 it is 2-way-coupled with the atmosphere and models the land surface processes at the same temporal and spatial resolution as the atmospheric model components of MM5. PROMET differs from MM5 both in temporal and spatial resolution. In order to couple PROMET with MM5, the coarse meteorological data provided by MM5 (45 × 45 km) has to be downscaled to the higher resolution of the land surface model (1 × 1 km) as well as the surface fluxes simulated by PROMET at a resolution of 1 km have to be upscaled to the MM5 model resolution. This is done by applying the scaling tool SCALMET (**Scal**ing **Met**eorological variables) (Marke, 2008; Marke et al., 2011a). SCALMET has been successfully applied in many 1-way coupled applications under a variety of hydro-meteorological boundary conditions e.g. in the Upper Danube Watershed in Europe (Marke, 2008; Marke et al., 2011a, b), in the Upper Brahmaputra Watershed in Asia (Prasch et al., 2011) or in the Gâtineau watershed in the US and Canada (Ludwig et al., 2009). In the framework of these studies, past as well as possible future hydrological scenarios have been simulated using PROMET with the meteorological drivers provided by different regional climate models (REMO, MM5, CLM, CRCM). The adjustable simulation time step within PROMET, which also constitutes the exchange time step between PROMET and MM5, is set to 9 min in the current study. This allows PROMET to run synchronously with MM5, which uses a time-step of 135 s. The statistical downscaling can either be used with regression based approaches (Daly et al., 2002) or empirical gradients (Liston and Elder, 2006), using elevation-dependencies in order to scale the meteorological data to the fine resolution grid.

In addition to the 1-way coupling in SCALMET, a 2-way coupling mode was designed and implemented by adding a linear upscaling of the scalar surface fluxes to SCALMET (see Fig. 5). In order to close the energy balance in the 2-way coupled land-atmosphere system, the downscaling as well as the upscaling approach for each variable is restricted to conserve mass and energy within the scaling processes in SCALMET. Hence, no bias correction is carried out in the framework of the model runs presented in this study. Therefore, any bias of the RCM is inevitably inherited by the LSM. The energy balance of the overall atmosphere-land-system is given as (Dingman, 2002):

$$\downarrow R_{\text{short}} + \downarrow R_{\text{long}} = \uparrow H_{\text{latent}} + \uparrow H_{\text{sensible}} + \uparrow R_{\text{long}} + \uparrow R_{\text{short}} + \downarrow H_{\text{ground}} \quad (10)$$

Where R_{short} and R_{long} are the incoming shortwave and logwave radiation that are partitioned into the latent heat flux (H_{latent}), the sensible heatflux (H_{sensible}) and the shortwave and longwave outgoing radiation (R_{short} and R_{long}) and the ground flux (H_{ground}).

HESSD
8, 7091–7136, 2011

5 Results and discussion

5.1 Comparing model evapotranspiration with equal meteorological drivers

Figure 6 shows the mean annual evapotranspiration from 1996–1999 simulated by the NOAH-LSM (left) and by PROMET (right), both models driven by the same atmospheric drivers.

Both models show a north to south gradient of evapotranspiration with lower values in the alpine region. The most obvious difference is the spatial heterogeneity related to the spatial resolution applied to each model. The PROMET evapotranspiration allows for recognizing small-scale spatial patterns such as alpine valleys with high contrasts to its surroundings and forested areas with high values of evapotranspiration as can be found in the Black Forest (approx. 48.5° N 8.3° E). While the PROMET land-use data set includes a number of impervious surfaces (such as residential or industrial areas and rocks) that do not contribute to transpiration and therefore reduce mean annual evapotranspiration, the NOAH underlying land-use data set accounts only for a small number of land-use classes and mainly implements cropland in the model domain (see Fig. 3). The effect of different land-uses and sealed surfaces in PROMET becomes especially apparent in large urban areas such as Berlin or the extended Ruhr region as well as in rocky alpine areas (see Fig. 6). In order to compare the model results on the same spatial scale, we aggregated the PROMET result to the spatial resolution of 45 × 45 km and finally subtracted it from the NOAH evapotranspiration (Fig. 7).

The overall mean annual evapotranspiration is lower in the PROMET simulation. Pixels with high percentage of impervious surfaces in PROMET such as Berlin (43 %), the Ruhr region (55 %) and Milan (37 %) show the highest differences of evapotranspiration (see Fig. 7) while the NOAH-LSM is parameterized with cropland in all those pixels (see Fig. 3). The simulated mean annual evapotranspiration for the Berlin pixels is 95 mm less per year in the PROMET simulation (260 mm) than in the NOAH simulation (355 mm), 183 mm less for the corresponding Ruhr pixels

HESSD
8, 7091–7136, 2011

(NOAH: 405 mm; PROMET: 222 mm) and even 283 mm less in the Milan pixels (NOAH: 707 mm; PROMET: 424 mm), which are the pixels with the largest difference.

Caused by the impervious surfaces in PROMET, annual transpiration contributes 56 % to evapotranspiration for the Milan pixels, 36 % for the Berlin pixels and 30 % for the pixels of the Ruhr region.

The effect of the different land-uses on simulated evapotranspiration can be investigated by comparing the temporal mean monthly behaviour of evapotranspiration (1996–1999) of the NOAH-LSM and the PROMET simulations.

Figure 7 takes a closer look at Milan and shows monthly NOAH-LSM and PROMET evapotranspiration exemplary for the 45 × 45 km Milan pixel, which contains 2025 different PROMET pixels. The PROMET land-use data for the 45 × 45 km MM5 Milan pixel contains 40 % residential and industrial pixels, 30 % forested areas and 30 % arable land within which 32 % are intensive grassland, 26 % are maize and silage (each 13 %) and 14 % are set-aside. The data was compiled from CORINE 2000 data combined with MERIS NDVI and EUROSTAT statistical data (Zabel et al., 2010). The PROMET results are displayed with and without the impervious PROMET pixels within the Milan MM5 pixel.

The prominent role of impervious surfaces in producing the average evapotranspiration can clearly be seen during the summer months, when NOAH-LSM and PROMET evapotranspiration differ largely when looking at the average evapotranspiration of all PROMET pixels of Milan. This difference in summer almost disappears when excluding the impervious pixels from the analysis and only taking the vegetated PROMET pixels into account. The annual difference in evapotranspiration between NOAH-LSM and PROMET is then reduced from about 200 mm to 86 mm. It is also remarkable that the largest differences, neglecting sealed surfaces within the PROMET simulation, occur in the spring months (March, April) and in summer (July, August).

While the NOAH-LSM uses monthly variations of the green vegetation fraction (σ_f) in order to take seasonal behaviour of vegetation into account, PROMET uses daily data of LAI, plant-height, albedo and root depth for each of its vegetation classes.

HESSD
8, 7091–7136, 2011

This results in a differentiated behaviour of evapotranspiration in PROMET in spring, since it is a mixture of large values of the developing cereal plants and small values for bare soil of open maize fields (which do not exist in NOAH-LSM). In summer cereals are harvested and maize is fully developing. Both during spring and summer vegetation fractions of NOAH-LSM and PROMET therefore differ. In winter differences are small since evapotranspiration is mainly energy and not land-use driven.

Figure 9 shows the comparison of the monthly development of the green vegetation fraction for the Milan pixel in the NOAH-LSM with the daily development of LAI for the most important land use classes for the corresponding PROMET pixels neglecting sealed surfaces. A prominent gap between the two model parameterizations can be recognized in springtime.

The monthly green vegetation fraction shows values of almost 40 % in April which means that 40 % of potential evaporation is possible in the NOAH-evapotranspiration approach. However, at the same time, the PROMET phenological development of deciduous forest and maize has not yet started and thus only the grassland and coniferous forested areas are contributing to transpiration. As a result, the PROMET monthly percentage of transpiration (15 mm) to evapotranspiration (44 mm) is about 30 % with respect to the vegetated Milan pixels in April.

In the summer months, vegetated stands are fully developed in both models but still, evapotranspiration rates for unsealed surfaces of PROMET are below those of the NOAH-LSM which is most likely due to water stress in the PROMET simulation that reduce summer plant transpiration rates. Since the water stress functions included in both models are not comparable due to different model approaches and different impacts on transpiration, Fig. 10 compares the daily course of simulated soil moisture between both models for the third soil layer representing the Milan pixel in the NOAH-LSM. The PROMET soil moisture is not averaged and exemplarily shown for a pixel vegetated with maize and parameterized with the soil type “loamy clay” in the 3rd soil layer which occurs most frequently (55 %) within the Milan area pixels, while MM5 is parameterized with soil type clay. The layer thickness reaches from 1 m to 2 m from

HESSD
8, 7091–7136, 2011

the land surface in the NOAH-LSM and reaches from 0.5 m to 1.5 m in PROMET. Soil properties describing water retention of the 3rd soil layer are most important in providing water for plant transpiration since maize is parameterized with a root fraction of 60 % within the 3rd soil layer in PROMET. The most important soil parameters within the NOAH-LSM that are necessary to determine water availability with respect to plant transpiration, are the maximum soil moisture (46.8 Vol-%. for the Milan pixel), the field capacity (41.2 Vol-%. soil moisture) and the wilting point (13.8 Vol-%. soil moisture).

Both models show a similar behaviour of soil moisture in the winter months. During the Mediterranean summer months, the soil moisture decreases in the NOAH simulation while it stops decreasing in the PROMET simulation reaching a threshold of 29 Vol-%. soil moisture each summer (see Fig. 10). This is due to the increasing soil suction in the "loamy clay" pixel and the reaction of maize to soil moisture deficit. Maize in PROMET is parameterized to react quite sensitively to increasing soil suction and starts restricting evapotranspiration at levels of soil suction of 0.8 MPa and completely closes stomata at 1.2 MPa, which is reached in the "loamy clay" soil at soil moisture levels of app. 29 Vol-%. This has a strong impact on the transpiration rate in the summer (see Fig. 11). The decrease in soil moisture within the NOAH simulation shows that soil water from the 3rd layer is still used for transpiration during the summer months, since the wilting point is parameterized with 13.8 Vol-% soil moisture. This value seems unusually low for an assumed clay soil in the MM5 soil dataset (see Fig. 11).

The development of the pF-value for the same PROMET sample-pixel is shown in Fig. 12. It is calculated as in PROMET after an approach of (Brooks and Corey, 1964) calculating the matrix potential // soil water potential (Ψ_s) as the following:

$$\Psi s = \Psi 1 \times S^{-1/m} \tag{11}$$

where Ψ_1 is the air entry tension (bubbling pressure head), S is the saturation of the effective pore space with water and m is the pore-size distribution index, which are all parameters also available within the soil parameterization of PROMET.

HESSD
8, 7091–7136, 2011

Inter-comparison of two land-surface schemes

F. Zabel et al.

Figure 12 demonstrates that the inhibition of transpiration is due to the increasing soil water potential in the 3rd soil layer. Maize is unable to suck more water out of the soil since the permanent wilting point is reached at the pF-value of about 4.2 when the soil moisture reaches less than 29 Vol-%.

5.2 Feedbacks to the atmosphere

The energy fluxes produced by both land surface models, as shown with the latent heat flux, affect the atmosphere in a complex way. In order to study the feedback effects between the coarse resolution regional climate model MM5 and the fine spatial resolution hydrologic land surface model PROMET, the models were coupled bilaterally (see Sect. 4). Therefore, PROMET is driven with MM5 atmosphere forcing and in return provides the lower boundary conditions for MM5 for each time step. Energy conservation is guaranteed within the coupled system. As a result, the atmosphere physics, simulated by MM5, are altered by the different lower boundary conditions. The impact of the fine spatial resolution land surface model PROMET on the atmosphere is investigated in the following.

Less transpiration in the bilaterally coupled PROMET simulation results in higher air temperature in comparison to the fully coupled NOAH simulation due to the fact that energy partitioning on the land surface is shifted from latent to sensible heat. The effect of less transpiration, due to impervious surfaces, can clearly be seen in the increased temperatures of the MM5 simulations fully coupled with PROMET e.g. for the Berlin or the Ruhr region (Fig. 13).

The changed lower boundary conditions in the PROMET land surface simulation also result in less annual precipitation amounts, especially in the Alpine area (see Fig. 14). While the spatial patterns of mean precipitation between NOAH-MM5 and PROMET-MM5 simulations are almost the same, total precipitation amounts decrease mostly north and south of the Alps and in the Po-Valley (up to 200 mm), where transpiration-rates in summer strongly decrease due to water-stress.

HESSD
8, 7091–7136, 2011

5.3 Feedbacks to the land surface

The changed atmospheric conditions in turn change the land surface energy fluxes. Figure 15 shows those feedback effects in terms of evapotranspiration. While increased temperature and decreased precipitation results in remarkably smaller evapotranspiration in the Po-Valley and South of the Alps, it results in the opposite effect namely in slightly increased evapotranspiration north of the Alps (see Fig. 15). Since in the Po-Valley, plant's water suctions already reached the wilting point in summer, the impact of less precipitation and increased temperature increases water-stress (see Fig. 16) and therefore inhibits evapotranspiration. On the other side, water-stress does not limit evapotranspiration north of the Alps since the positive effects on transpiration are predominant and still enough water is available for transpiration although precipitation amounts mainly decrease.

6 Conclusions

We compared the simulated evapotranspiration of two land surface models, both driven with the same meteorological data. As a result, the different behaviour of the two models regarding evapotranspiration was analyzed showing the greatest differences in the Po-Valley.

We identified three main reasons for the different simulation results. The first is the different spatial resolution that allows PROMET to account for spatial heterogeneity of the land surface (land-use, soil, elevation) in contrast to the coarse resolution applied in the NOAH-LSM. The most important impact on evapotranspiration is due to impervious surfaces that are contained in PROMET's high spatial resolution land-use data. They do not contribute to transpiration in PROMET while the NOAH-LSM is rather homogeneously classified with arable land. This result in lower evapotranspiration rates in PROMET compared to the NOAH-LSM especially in areas with a high degree of sealing.

Secondly, the role of plant parameterization in terms of phenological behaviour due to different model assumptions results in a temporal delay of PROMET evapotranspiration in spring for the Po-Valley. The NOAH-LSM uses the green vegetation fraction to account for seasonal behaviour of vegetation phenology. This parameter includes high uncertainties and seems to be more suitable for tuning rather than as a physical plant parameter. Nonetheless, the plant phenology parameterization of LAI, albedo, plant height and root length is homogeneously valid for each plant in PROMET. By replacing this fixed behaviour of vegetation phenology with a dynamic vegetation growth model the phenological behaviour of each could be adjusted to specific regions (Farquhar et al., 1980; Hank, 2008).

The third reason is related to different physical model approaches in terms of the soil and canopy treatment in both models. PROMET employs a more comprehensive treatment of biophysical and radiation interactions between soil surface, vegetation and the atmosphere and therefore has substantially more specified physical parameters than the NOAH-LSM. Therefore, water-stress in PROMET is the result of soil water potential and leaf water potential, thereby taking different plant specific properties into account while the NOAH-LSM considers it to be a function of soil water content only. We further showed that water-stress due to soil moisture availability results in less transpiration in PROMET, in particular in the Po-Valley.

The impact of the changed MM5 lower boundary by PROMET on the atmosphere was shown for near surface air temperature and precipitation. Both were significantly altered with different regional behaviour. The largest differences are found in the Po-Valley where annual temperature increased due to less evapotranspiration in PROMET while precipitation further decreased. The feedback with the atmosphere in turn also affects the land surface conditions. As a result, transpiration decreased due to lower soil moisture levels creating larger soil suction and a higher level of water-stress. Thus, this approach is able to take feedback effects between a high spatial resolution land surface model and a coarse resolution atmospheric model with a high level of detail into account. In a next step, simulation results of the bilaterally coupled PROMET-MM5 simulation shall be validated and tested against meteorological measurements for a specific area.

Overall, the role of parameterization in both models is characterized by two different ideologies. The models have historically been developed from different points of views and evolved from global to regional scale and from local to regional scale respectively. While the NOAH-LSM was originally designed for atmospheric applications, PROMET was developed to study hydrological issues on the local to regional scale. Therefore, in order to avoid "over-parameterization", the NOAH-LSM uses simplified parameters like the vegetation fraction with a high degree of uncertainty strongly affecting evapotranspiration. It is not designed to take important aspects of water-stress and plant specific transpiration into account. PROMET, on the other hand uses a large amount of plant and crop dependent parameters resulting in a spatially and temporally higher resolution, which however takes more computational resources.

Since plant transpiration controls biomass production and therefore yield, it is a critical and important parameter which spatial and temporal diversity depends on individual plant properties, the soil state and climate conditions. In terms of regional and local simulations of crop productivity, food-security and hydrological impact studies e.g. of water-stress due to climate change, the simplified approaches are not sufficient. More complex approaches are necessary that require a larger number of physical parameters for soil and individual plants. A variety of plant species and crop-types, with nonetheless a regional to global validity, need to be taken into account in order to simulate yields and in order to obtain a more realistic view of the heterogeneous land surface. Further, feedback effects from the land surface to the atmosphere within the sensible climate system are important issues in scientific research progress e.g. to study drought events that require an adequate and detailed description of land surface processes on the local and regional scale in terms of soil moisture and plant transpiration, affecting temperature and precipitation behaviour of the atmosphere.

HESSD
8, 7091–7136, 2011

Acknowledgements. The research described in this paper was carried out at the Department of Geography of the Ludwig Maximilians Universität in Munich, Germany as part of the GLOWA-Danube project, which was funded by BMBF from 2000 to 2010. The support is gratefully acknowledged.

References

Bach, H. and Verhoef, W.: Sensitivity studies on the effect of surface soil moisture on canopy reflectance using the radiative transfer model GeoSAIL, Igarss 2003: Ieee International Geoscience and Remote Sensing Symposium, Vols I–Vii, Proceedings, 1679–1681, 2003.

Baldocchi, D. D., Hicks, B. B., and Camara, P.: A canopy stomatal resistance model for gaseous deposition to vegetated surfaces, Atmospheric Environment (1967), 21, 91–101, doi:10.1016/0004-6981(87)90274-5, 1987.

Bharati, L., Rodgers, C., Erdenberger, T., Plotnikova, M., Shumilov, S., Vlek, P., and Martin, N.: Integration of economic and hydrologic models: Exploring conjunctive irrigation water use strategies in the Volta Basin, Agr. Water Manag., 95, 925–936, doi:10.1016/j.agwat.2008.03.009, 2008.

Biscoe, P. V., Cohen, Y., and Wallace, J. S.: Daily and Seasonal Changes of Water Potential in Cereals, Philos. T. Royal Soc. B, 273, 565-580, 1976.

Bonan, G. B.: Land-Atmosphere interactions for climate system Models: coupling biophysical, biogeochemical, and ecosystem dynamical processes, Remote Sens. Environ., 51, 57–73, doi:10.1016/0034-4257(94)00065-u, 1995.

Bounoua, L., Collatz, G. J., Los, O. S., Sellers, P. J., Dazlich, D. A., Tucker, C. J., and Randall, D. A.: Sensitivity of Climate Changes in NDVI, J. Climate, 13, 2277–2292, 2000.

Brooks, R. H. and Corey, A. T.: Hydraulic properties of porous media, Colorado State University, 1964.

Campbell, G. S. and Norman, J. M.: An Introduction To Environmental Biophysics, 2 Edn, Springer, New York, 2000.

Chen, F. and Dudhia, J.: Coupling an Advanced Land Surface – Hydrology Model with the Penn State–NCAR MM5 Modeling System. Part I: Model Implementation and Sensitivity, Mon. Weather Rev., 129, 569–585, 2001a.

Chen, F. and Dudhia, J.: Coupling an Advanced Land Surface–Hydrology Model with the Penn

HESSD
8, 7091–7136, 2011

State–NCAR MM5 Modeling System. Part II: Preliminary Model Validation, Mon. Weather Rev., 129, 587–604, 2001b.
Chen, F., Mitchell, K., Schaake, J., Xue, Y., Pan, H.-L., Koren, V., Duan, Q. Y., Ek, M., and Betts, A.: Modeling of land surface evaporation by four schemes and comparison with FIFE observations, J. Geophys. Res., 101(D3), 7251–7268, doi:10.1029/95JD02165, 1996.
Daly, C., Gibson, W. P., Taylor, G. H., Johnson, G. L., and Pasteris, P.: A knowledgebased approach to the statistical mapping of climate, Clim. Res., 22(14), 99–113, 2002.
Devonec, E. and Barros, A. P.: Exploring the transferability of a land-surface hydrology model, J. Hydrol., 265, 258–282, doi:10.1016/s0022-1694(02)00111-7, 2002.
Dickinson, R. E.: Land processes in climate models, Remote Sens. Environ., 51, 27–38, doi:10.1016/0034-4257(94)00062-r, 1995.
Dickinson, R. E., Henderson-Sellers, A., Rosenzweig, C., and Sellers, P. J.: Evapotranspiration models with canopy resistance for use in climate models, a review, Agr. Forest Meteorol., 54, 373–388, doi:10.1016/0168-1923(91)90014-h, 1991.
Dingman, S. L.: Physical Hydrology, Prentice Hall, New Jersey, 2002.
Essery, R. L. H., Best, M. J., Betts, R. A., and Cox, P. M.: Explicit Representation of Subgrid Heterogeneity in a GCM Land Surface Scheme, J. Hydrometeorol., 4, 530–543, 2003.
Famiglietti, J. S. and Wood, E. F.: Evapotranspiration and runoff from large land areas: Land surface hydrology for atmospheric general circulation models, Surv. Geophys., 12, 179–204, doi:10.1007/bf01903418, 1991.
Farquhar, G. D., Caemmerer, S. V., and Berry, J. A.: A biochemical-model of photosynthetic CO_2 assimilation in leaves of c-3 species, Planta, 149, 78–90, 1980.
Garcia-Quijano, J. F. and Barros, A. P.: Incorporating canopy physiology into a hydrological model: photosynthesis, dynamic respiration, and stomatal sensitivity, Ecol. Model., 185, 29–49, doi:10.1016/j.ecolmodel.2004.08.024, 2005.
Ge, J., Qi, J., Lofgren, B. M., Moore, N., Torbick, N., and Olson, J. M.: Impacts of land use/cover classification accuracy on regional climate simulations, J. Geophys. Res., 112, D05107, doi:10.1029/2006JD007404, 2007.
Gutman, G. and Ignatov, A.: Satellite-derived green vegetation fraction for the use in numerical weather prediction models, Adv. Space Res., 19, 477–480, doi:10.1016/s0273-1177(97)00058-6, 1997.
Hagemann, S., Botzet, M., and Machenhauer, B.: The summer drying problem over southeastern europe: sensitivity of the limited area model HIRHAM4 to improvements in physical

HESSD
8, 7091–7136, 2011

parameterization and resolution, Phys. Chem. Earth, Pt B, 26, 391–396, doi:10.1016/s1464-1909(01)00024-7, 2001.
Hank, T. B.: A Biophysically Based Coupled Model Approach For the Assessment of Canopy Processes Under Climate Change Conditions, Fakultät für Geowissenschaften, Ludwig-Maximilians-Universität, München, 2008.
Henderson-Sellers, A., Dickinson, R. E., and Pitman, A. J.: Atmosphere-landsurface modelling, Math. Comput. Model., 21, 5–10, doi:10.1016/0895-7177(95)00045-4, 1995.
Henderson-Sellers, A., McGuffie, K., and Pitman, A. J.: The Project for Intercomparison of Land-surface Parametrization Schemes (PILPS): 1992 to 1995, Clim. Dynam., 12, 849–859, 1996.
Henderson-Sellers, A., Irannejad, P., and McGuffie, K.: Future desertification and climate change: The need for land-surface system evaluation improvement, Global Planet. Change, 64, 129–138, doi:10.1016/j.gloplacha.2008.06.007, 2008.
Jacob, D., Bärring, L., Christensen, O. B., Christensen, J. H., Castro, M. D., Déqué, M., Giorgi, F., Hagemann, S., Hirschi, M., Jones, R., Kjellström, E., Lenderink, G., Rockel, B., Sánchez, E., Schär, C., Seneviratne, S. I., Somot, S., Ulden, A. v., and Hurk, B. v. d.: An inter-comparison of regional climate models for Europe: model performance in present-day climate, Climatic Change, 81, 31–52, doi:10.1007/s10584-006-9213-4, 2007.
Jacquemin, B. and Noilhan, J.: Sensitivity study and validation of a land surface parameterization using the HAPEX-MOBILHY data set, Bound.-Lay. Meteorol., 52, 93–134, doi:10.1007/bf00123180, 1990.
Jarvis, P. G.: The Interpretation of the Variations in Leaf Water Potential and Stomatal Conductance Found in Canopies in the Field, Philos. T. R. Soc. Lon., 273, 593-610, 1976.
Koster, R. D. and Suarez, M. J.: The components of a 'SVAT' scheme and their effects on a GCM's hydrological cycle, Adv. Water Res., 17, 61–78, doi:10.1016/0309-1708(94)90024-8, 1994.
Koster, R. D., Dirmeyer, P. A., Guo, Z. C., Bonan, G., Chan, E., Cox, P., Gordon, C. T., Kanae, S., Kowalczyk, E., Lawrence, D., Liu, P., Lu, C. H., Malyshev, S., McAvaney, B., Mitchell, K., Mocko, D., Oki, T., Oleson, K., Pitman, A., Sud, Y. C., Taylor, C. M., Verseghy, D., Vasic, R., Xue, Y. K., Yamada, T., and Team, G.: Regions of strong coupling between soil moisture and precipitation, Science, 305, 1138-1140, 2004.
Kuchment, L. S., Demidov, V. N., and Startseva, Z. P.: Coupled modeling of the hydrological and carbon cycles in the soil-vegetation-atmosphere system, J. Hydrol., 323, 4–21,

doi:10.1016/j.jhydrol.2005.08.011, 2006.
Kueppers, L. M., Snyder, M. A., Sloan, L. C., Cayan, D., Jin, J., Kanamaru, H., Kanamitsu, M., Miller, N. L., Tyree, M., Du, H., and Weare, B.: Seasonal temperature responses to land-use change in the western United States, Global Planet. Change, 60, 250–264, doi:10.1016/j.gloplacha.2007.03.005, 2008.
Kunstmann, H., Jung, G., Wagner, S., and Clottey, H.: Integration of atmospheric sciences and hydrology for the development of decision support systems in sustainable water management, Phys. Chem. Earth, Parts A/B/C, 33, 165–174, doi:10.1016/j.pce.2007.04.010, 2008.
Laprise, R.: Regional climate modelling, J. Comput. Phys., 227, 3641–3666, doi:10.1016/j.jcp.2006.10.024, 2008.
Liston, G. E. and Elder, K.: A Meteorological Distribution System for High-Resolution Terrestrial Modeling (MicroMet), J. Hydrometeorol., 7(17), 217–237, 2006.
Loew, A.: Impact of surface heterogeneity on surface soil moisture retrievals from passive microwave data at the regional scale: The Upper Danube case, Remote Sens. Environ., 112, 231–248, doi:10.1016/j.rse.2007.04.009, 2008.
Loew, A., Holmes, T., and Jeu, R. d.: The European heat wave 2003: early indicators from multisensoral microwave remote sensing?, J. Geophys. Res., 114, D05103, doi:10.1029/2008JD010533, 2009.
Ludwig, R. and Mauser, W.: Modelling catchment hydrology within a GIS based SVAT-model framework, Hydrol. Earth Syst. Sci., 4, 239–249, doi:10.5194/hess-4-239-2000, 2000.
Ludwig, R., Probeck, M., and Mauser, W.: Mesoscale water balance modelling in the Upper Danube watershed using sub-scale land cover information derived from NOAA-AVHRR imagery and GIS-techniques, Phys. Chem. Earth, Parts A/B/C, 28, 1351–1364, doi:10.1016/j.pce.2003.09.011, 2003a.
Ludwig, R., Taschner, S., and Mauser, W.: Modelling floods in the Ammer catchment: limitations and challenges with a coupled meteo-hydrological model approach, Hydrol. Earth Syst. Sci., 7, 833–847, doi:10.5194/hess-7-833-2003, 2003b.
Ludwig, R., May, I., Turcotte, R., Vescovi, L., Braun, M., Cyr, J.-F., Fortin, L.-G., Chaumont, D., Biner, S., Chartier, I., Caya, D., and Mauser, W.: The role of hydrological model complexity and uncertainty in climate change impact assessment, Adv. Geosci., 21, 63–71, 2009, http://www.adv-geosci.net/21/63/2009/.
Mahrt, L. and Ek, M.: The Influence of Atmosperic Stability on Potential Evaporation, J. Clim. Appl. Meteorol., 23, 222–234, 1984.

Marke, T.: Development and Application of a Model Interface To couple Land Surface Models with Regional Climate Models For Climate Change Risk Assessment In the Upper Danube Watershed, Fakultät für Geowissenschaften, Ludwig-Maximilians-Universität, München, 2008.
Marke, T., Mauser, W., Pfeiffer, A., and Zängl, G.: A pragmatic approach for the downscaling and bias correction of regional climate simulations evaluation in hydrological modeling, Geosci. Model Dev. Discuss., 4, 45–63, doi:10.5194/gmdd-4-45-2011, 2011a.
Marke, T., Mauser, W., Pfeiffer, A., Zängl, G., and Jacob, D.: The effect of downscaling on river runoff modeling: a hydrological case study in the Upper Danube Watershed, Hydrol. Earth Syst. Sci. Discuss., 8, 6331–6384, doi:10.5194/hessd-8-6331-2011, 2011b.
Martin, P. H.: Land-surface characterization in climate models: biome-based parameter inference is not equivalent to local direct estimation, J. Hydrol., 212–213, 287–303, doi:10.1016/s0022-1694(98)00212-1, 1998.
Mauser, W. and Bach, H.: PROMET – Large scale distributed hydrological modelling to study the impact of climate change on the water flows of mountain watersheds, J. Hydrol., 376, 362–377, doi:10.1016/j.jhydrol.2009.07.046, 2009.
Mauser, W. and Schädlich, S.: Modelling the spatial distribution of evapotranspiration on different scales using remote sensing data, J. Hydrol., 212–213, 250–267, doi:10.1016/s0022-1694(98)00228-5, 1998.
Mc Gregor, J. L.: Regional Climate Modelling, Meterol. Atmos. Phys., 63, 105–117, 1997.
Michalakes, J.: MM90: A scalable parallel implementation of the Penn State/NCAR Mesoscale Model (MM5), Parallel Comput., 23, 2173–2186, 1997.
Mitchell, K.: The Community Noah Land-Surface Model (LSM), 2005.
Molod, A. and Salmun, H.: A global assessment of the mosaic approach to modeling land surface heterogeneity, J. Geophys. Res., 107, 4217, doi:10.1029/2001jd000588, 2002.
Monteith, J. L.: Evaporation and the environment, Sym. Soc. Exp. Biol., 19, 205–234, 1965.
Monteith, J. L. and Unsworth, M. H.: Principles of Environmental Physics, 3 Edn, Elsevier, New York, 2008.
Muerth, M. J.: A Soil Temperature and Energy Balance Model for Integrated Assessment of Global Change Impacts at the regional scale, Fakultät für Geowissenschaften, Ludwig-Maximilians-Universität, München, 2008.
Noilhan, J. and Planton, S.: A Simple Parameterization of Land Surface Processes for Meteorological Models, Mon. Weather Rev., 117(14), 536–550, 1989.

HESSD
8, 7091–7136, 2011

Orlowsky, B. and Seneviratne, S. I.: Statistical Analyses of Land–Atmosphere Feedbacks and Their Possible Pitfalls, J. Climate, 23, 3918–3932, 2010.
Pfeiffer, A. and Zängl, G.: Validation of climate-mode MM5-simulations for the European Alpine Region, Theoretical Applied Climatology, 101, 93–108, doi:10.1007/s00704-009-0199-5, 2009.
Pitman, A. J.: The evolution of, and revolution in, land surface schemes designed for climate models, Int. J. Climatol., 23, 479–510, doi:10.1002/joc.893, 2003.
Polcher, J., McAvaney, B., Viterbo, P., Gaertner, M. A., Hahmann, A., Mahfouf, J. F., Noilhan, J., Phillips, T., Pitman, A., Schlosser, C. A., Schulz, J. P., Timbal, B., Verseghy, D., and Xue, Y.: A proposal for a general interface between land surface schemes and general circulation models, Global Planet. Change, 19, 261–276, doi:10.1016/s0921-8181(98)00052-6, 1998.
Prasch, M., Strasser, U., and Mauser, W.: Validation of a physically based snow model for the simulation of the accumulation and ablation of snow (ESCIMO). in: Berchtesgaden National Park Research Report Proceedings of the Alpine Snow Workshop, Munich, 2006.
Prasch, M., Marke, T., Strasser, U., and Mauser, W.: Large scale integrated hydrological modelling of the impact of climate change on the water balance with DANUBIA, Adv. Sci. Res., 7(9), 61–70, doi:10.5194/asr-7-61-2011, 2011.
Quintanar, A. I., Mahmood, R., Motley, M. V., Yan, J., Loughrin, J., and Lovanh, N.: Simulation of boundary layer trajectory dispersion sensitivity to soil moisture conditions: MM5 and Noah-based investigation, Atmos. Environ., 43, 3774–3785, doi:10.1016/j.atmosenv.2009.04.005, 2009.
Richter, K. and Timmermans, W. J.: Physically based retrieval of crop characteristics for improved water use estimates, Hydrol. Earth Syst. Sci., 13, 663–674, doi:10.5194/hess-13-663-2009, 2009.
Schaake, J. C., Koren, V. I., Duan, Q.-Y., Mitchell, K., and Chen, F.: Simple water balance model for estimating runoff at different spatial and temporal scales, J. Geophys. Res., 101, 7461–7475, doi:10.1029/95jd02892, 1996.
Schär, C., Vidale, P. L., Lüthi, D., Frei, C., Häberli, C., Liniger, M. A., and Appenzeller, C.: The role of increasing temperature variability in European summer heatwaves, Nature, 427, 332–336, 2004.
Schulla, J. and Jasper, K.: Model description of WaSiM-ETH, Institute of Geography, ETH Zürich, 1999.
Seth, A., Giorgi, F., and Dickinson, R. E.: Simulating fluxes from heterogeneous land surfaces

– explicit subgrid method employing the biosphere-atmosphere transfer scheme (BATS), J. Geophys. Res.-Atmos., 99, 18651–18667, 1994.
Stocker, T.: Einführung in die Klimamodellierung, Universität Bern, Bern, 2004.
Strasser, U. and Mauser, W.: Modelling the Spatial and Temporal Variations of the Water Balance for the Weser Catchment 1965-1994, J. Hydrol., 254, 199–214, 2001.
Strasser, U., Franz, H., and Mauser, W.: Distributed modelling of snow processes in the Berchtesgaden National Park (Germany), in: Berchtesgaden National Park Research Report Proceedings of the Alpine Snow Workshop, Munich, 117–130, 2007.
Timbal, B. and Henderson-Sellers, A.: Intercomparisons of land-surface parameterizations coupled to a limited area forecast model, Global Planet. Change, 19, 247–260, doi:10.1016/s0921-8181(98)00051-4, 1998.
Uppala, S. M., Kallberg, P. W., Simmons, A. J., Andrae, U., Bechtold, V. D. C., Fiorino, M., Gibson, J. K., Haseler, J., Hernandez, A., Kelly, G. A., Li, X., Onogi, K., Saarinen, S., Sokka, N., Allan, R. P., Andersson, E., Arpe, K., Balmaseda, M. A., Beljaars, A. C. M., Berg, L. V. D., Bidlot, J., Bormann, N., Caires, S., Chevallier, F., Dethof, A., Dragosavac, M., Fisher, M., Fuentes, M., Hagemann, S., Hólm, E., Hoskins, B. J., Isaksen, L., Janssen, P. A. E. M., Jenne, R., McNally, A. P., Mahfouf, J.-F., Morcrette, J.-J., Rayner, N. A., Saunders, R. W., Simon, P., Sterl, A., Trenberth, K. E., Untch, A., Vasiljevic, D., Viterbo, P., and Woollen, J.: The ERA-40 Re-analysis., Q. J. Roy. Meteorol. So., 131, 2961–3012, doi:10.1256/qj.04.176, 2005.
Wagner, S., Kunstmann, H., Bárdossy, A., Conrad, C., and Colditz, R. R.: Water balance estimation of a poorly gauged catchment in West Africa using dynamically downscaled meteorological fields and remote sensing information, Phys. Chem. Earth, Parts A/B/C, 34, 225–235, doi:10.1016/j.pce.2008.04.002, 2009.
Weber, M., Braun, L., Mauser, W., and M., P.: Contribution of rain, snow- and icemelt in the Upper Danube discharge today and in the future, Geogr. Fis. Din. Quat., 33, 221–230, 2010.
Wood, E. F., Lettenmaier, D. P., Liang, X., Lohmann, D., Boone, A., Chang, S., Chen, F., Dai, Y., Dickinson, R. E., Duan, Q., Ek, M., Gusev, Y. M., Habets, F., Irannejad, P., Koster, R., Mitchel, K. E., Nasonova, O. N., Noilhan, J., Schaake, J., Schlosser, A., Shao, Y., Shmakin, A. B., Verseghy, D., Warrach, K., Wetzel, P., Xue, Y., Yang, Z.-L., and Zeng, Q.-C.: The Project for Intercomparison of Land-surface Parameterization Schemes (PILPS) Phase 2(c) Red-Arkansas River basin experiment:: 1. Experiment description and summary intercomparisons, Global Planet. Change, 19, 115–135, doi:10.1016/s0921-8181(98)00044-7, 1998.

Yang, Z.-L., Dickinson, R. E., Shuttleworth, W. J., and Shaikh, M.: Treatment of soil, vegetation and snow in land surface models: a test of the Biosphere-Atmosphere Transfer Scheme with the HAPEX-MOBILHY, ABRACOS and Russian data, J. Hydrol., 212–213, 109–127, doi:10.1016/s0022-1694(98)00205-4, 1998.

Yu, Z.: Assessing the response of subgrid hydrologic processes to atmospheric forcing with a hydrologic model system, Global Planet. Change, 25, 1–17, doi:10.1016/s0921-8181(00)00018-7, 2000.

Zabel, F., Hank, T. B., and Mauser, W.: Improving arable land heterogeneity information in available land cover products for land surface modelling using MERIS NDVI data, Hydrol. Earth Syst. Sci., 14, 2073–2084, doi:10.5194/hess-14-2073-2010, 2010.

Zampieri, M., Giorgi, F., Lionello, P., and Nikulin, G.: Regional climate change in the Northern Adriatic, Physics. Chem. Earth, Parts A/B/C, in Press, Corrected Proof, doi:10.1016/j.pce.2010.02.003, 2011.

Zängl, G.: An improved method for computing horizontal diffusion in a sigma-coordinate model and its application to simulations over mountainous topography., Mon. Weather Rev., 130, 1423–1432, 2002.

Zeng, X. M., Zhao, M., Su, B. K., Tang, J. P., Zheng, Y. Q., Zhang, Y. J., and Chen, J.: Effects of the land-surface heterogeneities in temperature and moisture from the "combined approach" on regional climate: a sensitivity study, Global Planet. Change, 37, 247–263, doi:10.1016/s0921-8181(02)00209-6, 2003.

HESSD
8, 7091–7136, 2011

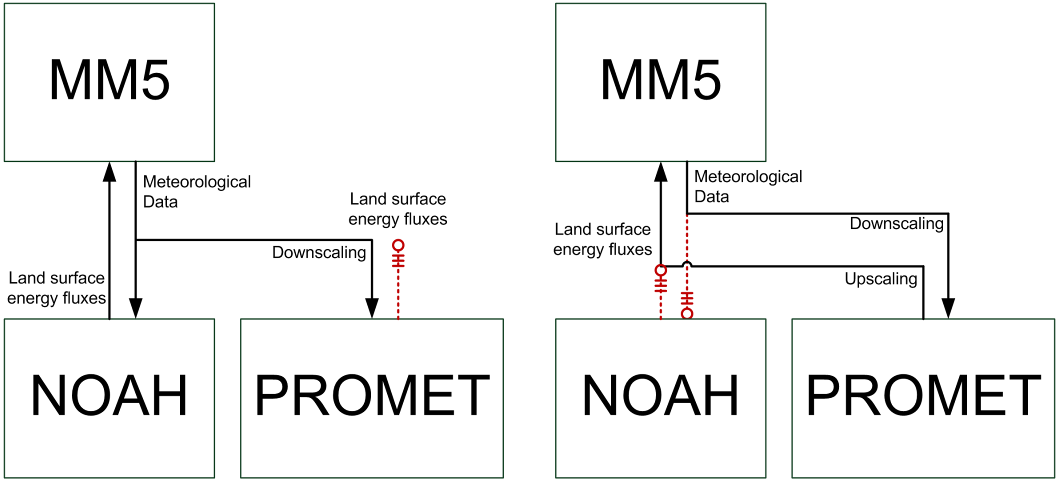

Fig. 1. Schematic illustration of model setup using the same atmosphere forcings for both land surface models (left) and in case of taking PROMET feedback effects into account (right). Red coloured lines indicate non-coupled fluxes.

HESSD
8, 7091–7136, 2011

Inter-comparison of two land-surface schemes

F. Zabel et al.

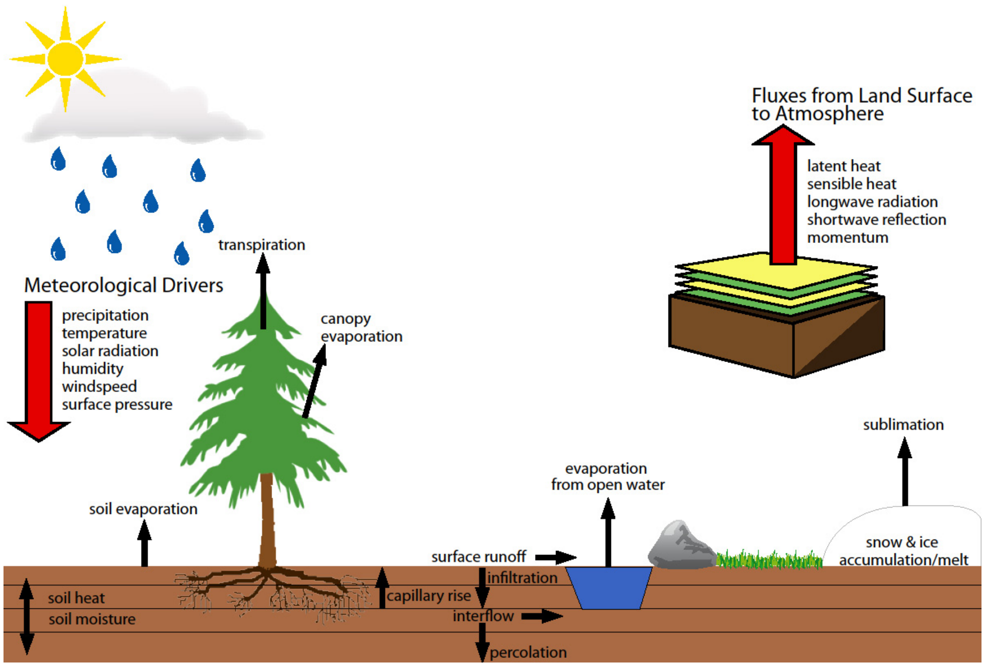

Fig. 2. Scheme of water and energy fluxes on the land surface and feedbacks to the atmosphere.

HESSD
8, 7091–7136, 2011

Inter-comparison of two land-surface schemes

F. Zabel et al.

Title Page
Abstract | Introduction
Conclusions | References
Tables | Figures
◀ | ▶
Back | Close
Full Screen / Esc
Printer-friendly Version
Interactive Discussion

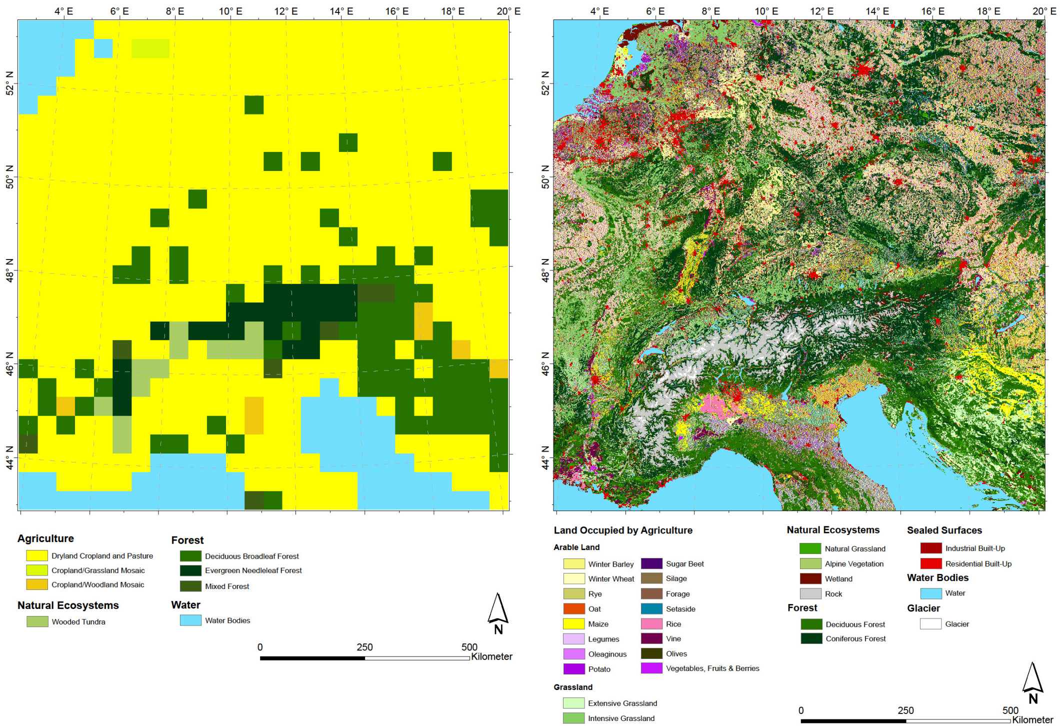

Fig. 3. Land use classification of the NOAH-LSM (45 × 45 km) and of PROMET (1x1 km).

HESSD
8, 7091–7136, 2011

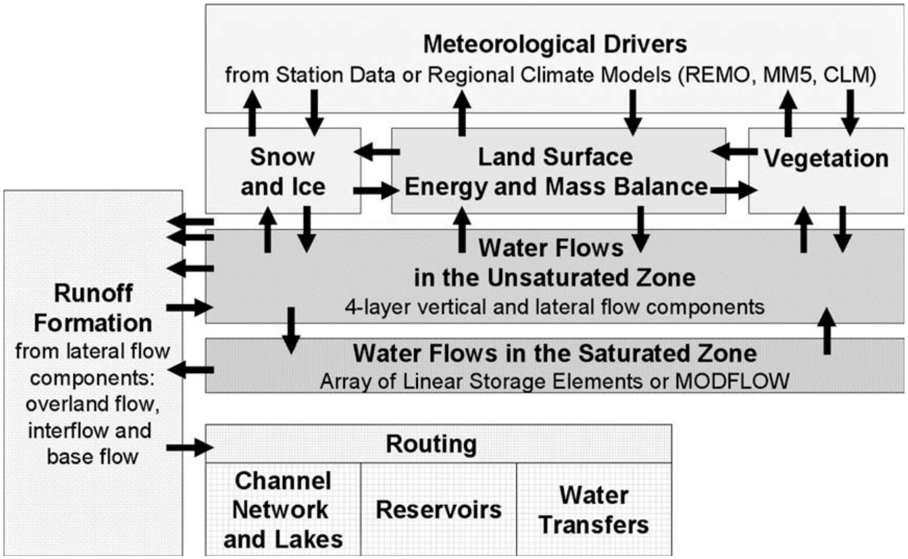

Fig. 4. Model components of PROMET.

HESSD
8, 7091–7136, 2011

Inter-comparison of two land-surface schemes

F. Zabel et al.

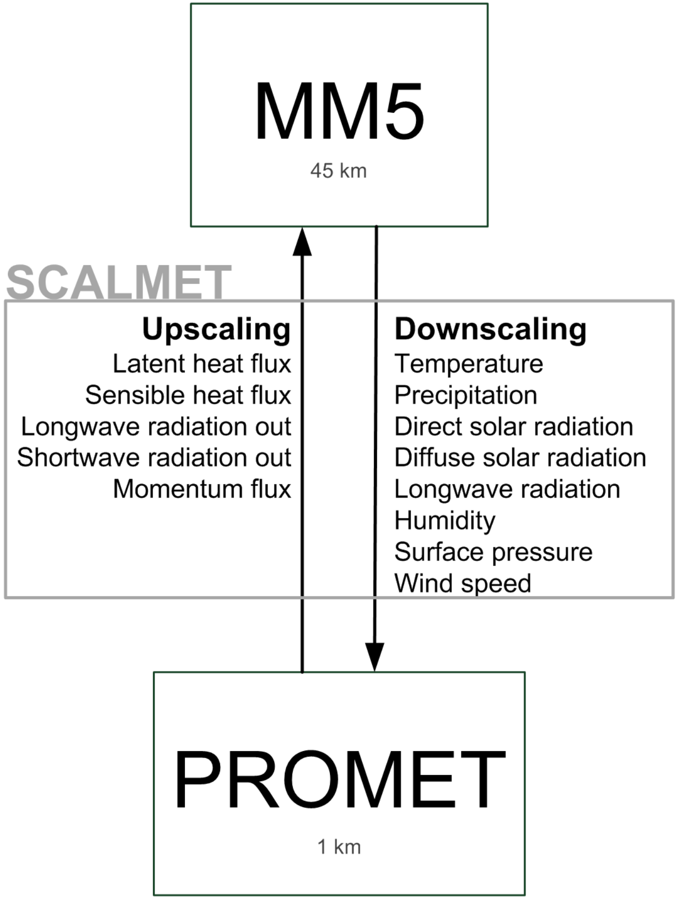

Fig. 5. The model setup of 2-Way-Coupling MM5 and PROMET using the scaling interface SCALMET.

HESSD
8, 7091–7136, 2011

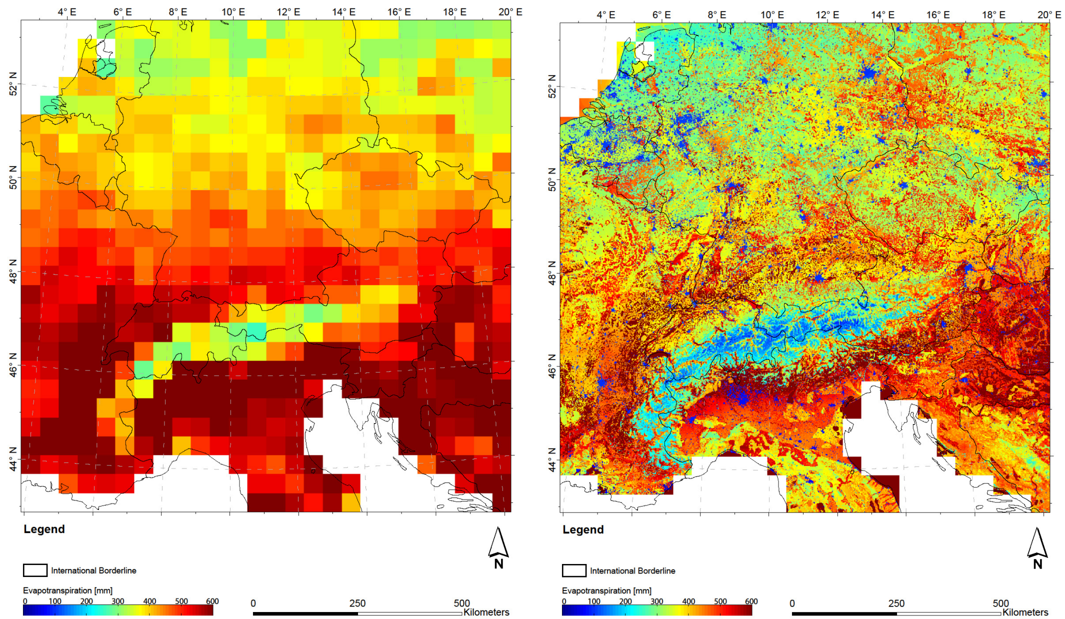

Fig. 6. Mean annual evapotranspiration of NOAH-LSM (left) and PROMET (right), both driven with the same MM5 meteorology.

HESSD
8, 7091–7136, 2011

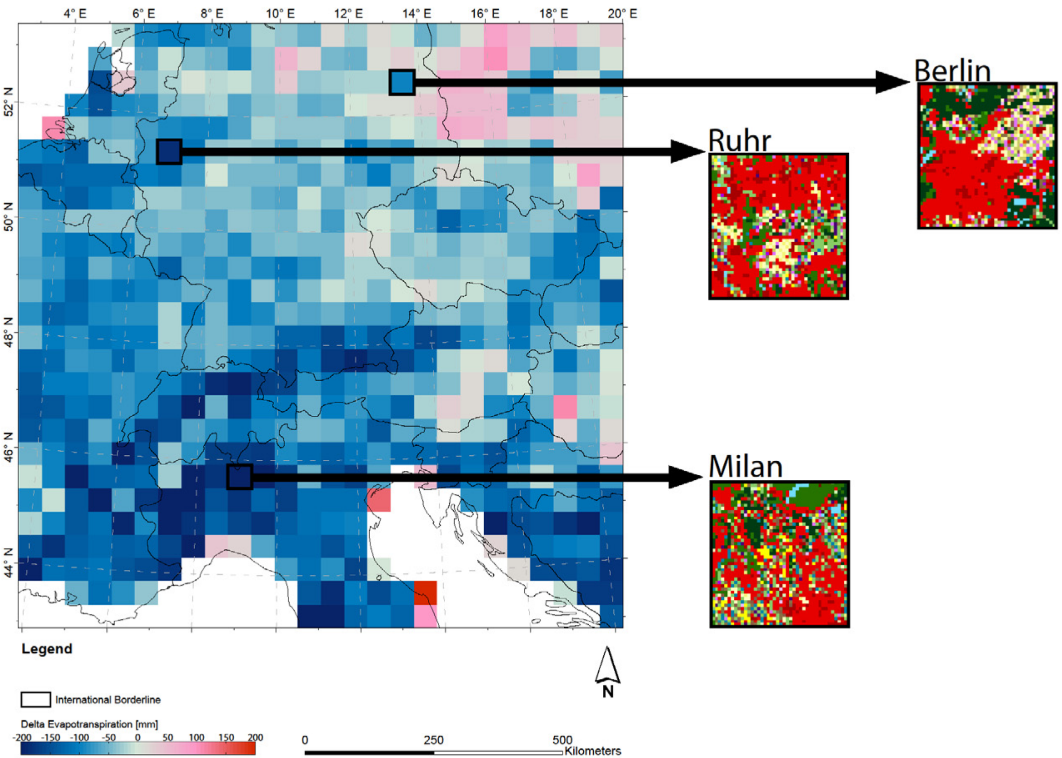

Fig. 7. Difference plot of mean annual evapotranspiration of PROMET - NOAH-LSM driven by the same meteorological data and exemplary compared to 1 km^2 land use (legend see Fig. 3) for the Berlin, Ruhr and Milan pixel (red indicates urban areas).

HESSD
8, 7091–7136, 2011

Inter-comparison of two land-surface schemes

F. Zabel et al.

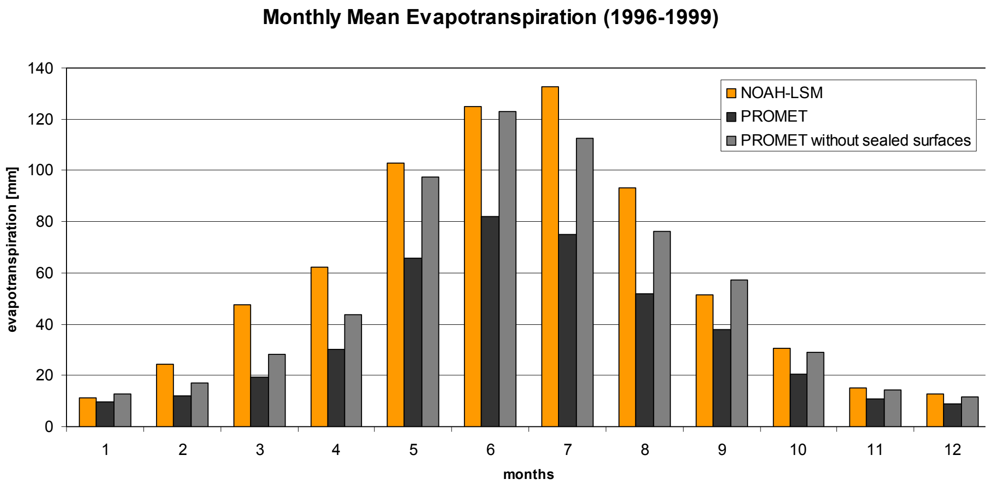

Fig. 8. Monthly mean evapotranspiration from 1996 - 1999 for the Milan Pixel of the NOAH-LSM and all corresponding PROMET pixels respectively masked without sealed surfaces, only accounting vegetated pixels.

HESSD
8, 7091–7136, 2011

Inter-comparison of two land-surface schemes

F. Zabel et al.

Title Page
Abstract
Introduction
Conclusions
References
Tables
Figures
◀◀
▶▶
◀
▶
Back
Close
Full Screen / Esc
Printer-friendly Version
Interactive Discussion

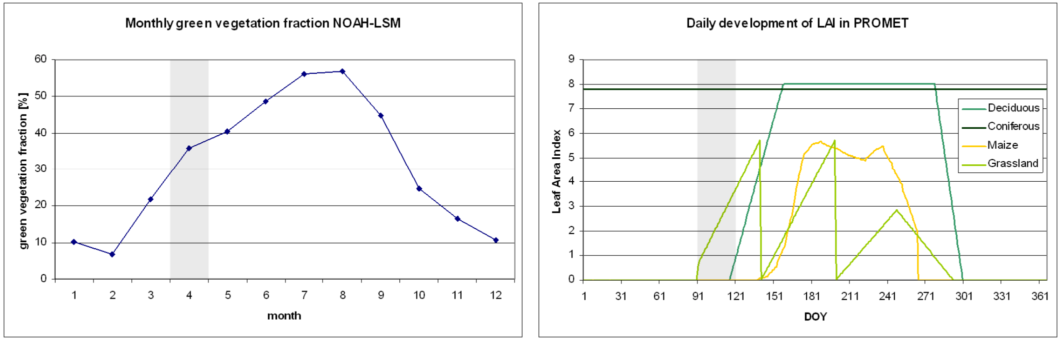

Fig. 9. NOAH-LSM development of the green vegetation fraction of the considered Pixel in the Po-valley and daily LAI development for deciduous forest, maize and grassland in PROMET.

HESSD
8, 7091–7136, 2011

Title Page
Abstract | Introduction
Conclusions | References
Tables | Figures
◀◀ | ▶▶
◀ | ▶
Back | Close
Full Screen / Esc
Printer-friendly Version
Interactive Discussion

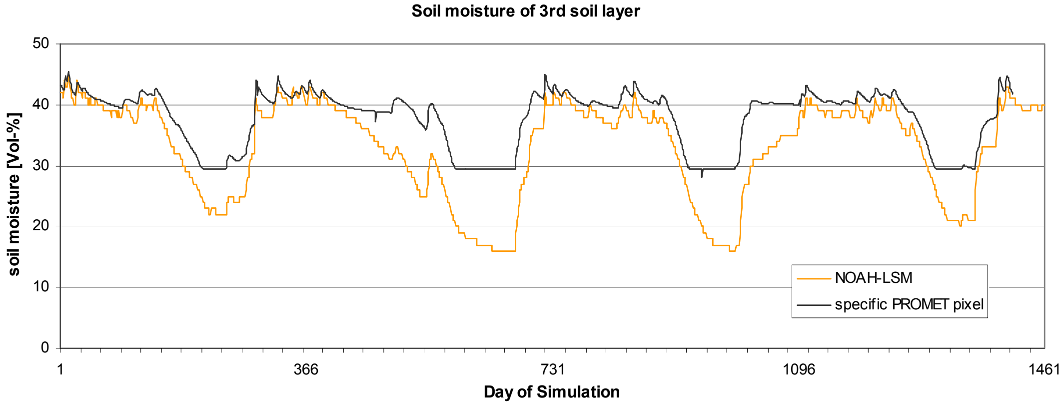

Fig. 10. Daily soil moisture (1996–1999) of the 3rd soil layer simulated by the NOAH-LSM for the Milan 45 km^2 pixel and by PROMET exemplarily for one 1 km^2 pixel inside the Milan area with land-use maize and soil type "loamy clay" in the 3rd soil layer.

HESSD
8, 7091–7136, 2011

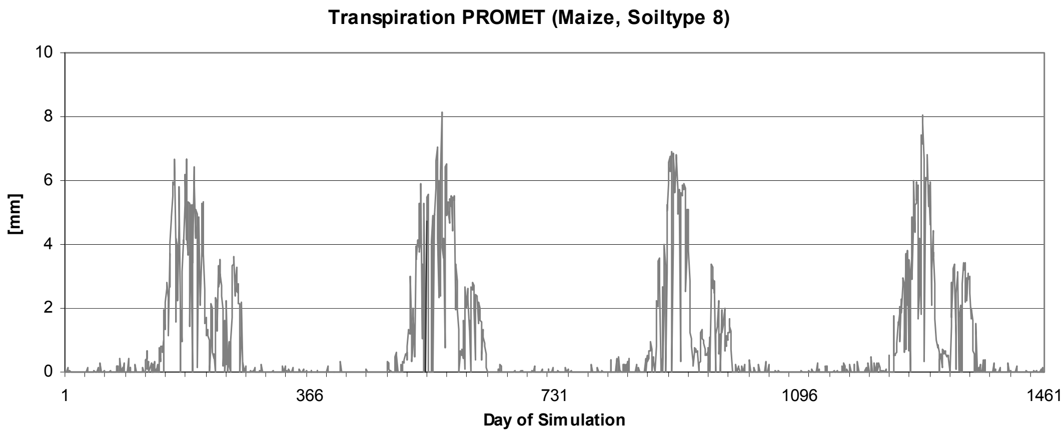

Fig. 11. Daily transpiration (1996–1999) simulated by PROMET exemplarily for one 1 km^2 pixel with land-use maize and soil type "loamy clay" in the 3rd soil layer.

HESSD
8, 7091–7136, 2011

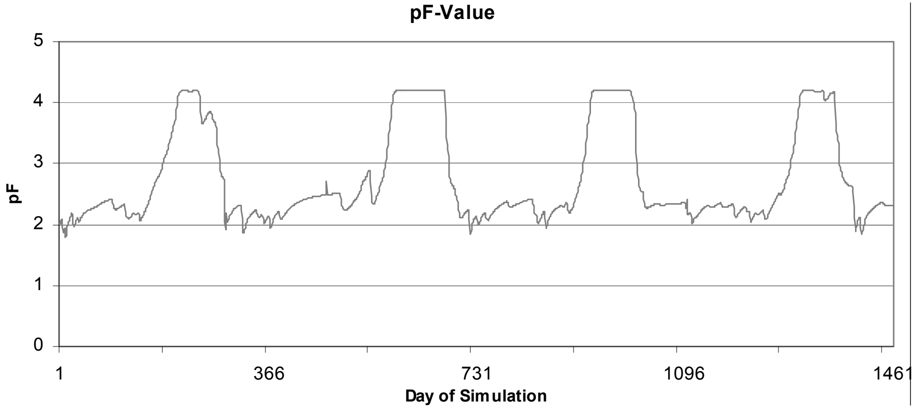

Fig. 12. Daily pF-value (1996–1999) simulated by PROMET exemplarily for one 1 km^2 pixel with land-use maize and soil type "loamy clay" in the 3rd soil layer.

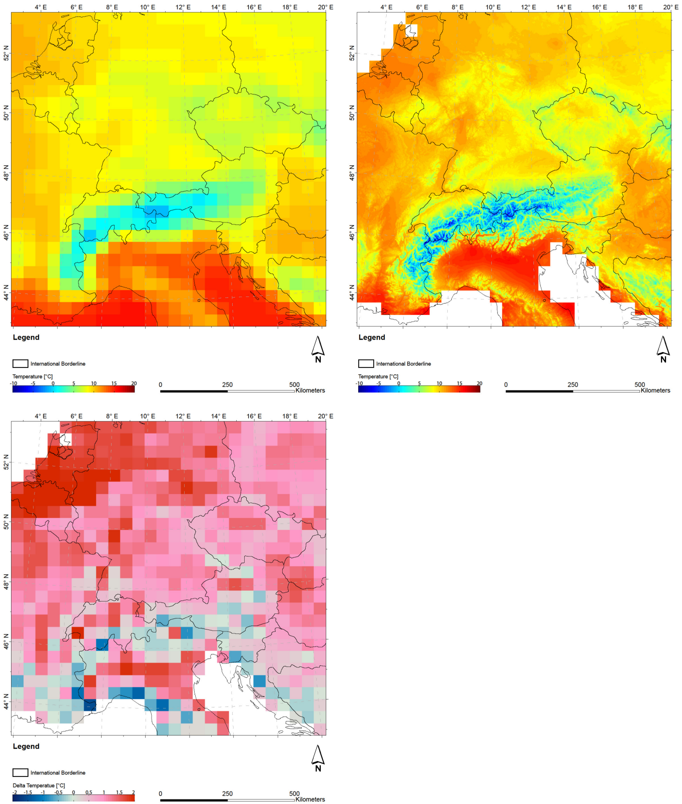

Fig. 13. Mean annual near surface air temperature [°C] (01.01.1996–31.12.1999) of MM5 simulations, fully coupled with the NOAH-LSM for providing the lower boundary conditions at a spatial resolution of 45 km (upper left) and fully coupled with PROMET at a spatial resolution of 1 km (upper right). Subtraction image, generated by aggregating fluxes from 1 × 1 km to 45 × 45 km, of fully coupled PROMET and fully coupled NOAH-LSM simulation (lower left).

HESSD

8, 7091–7136, 2011

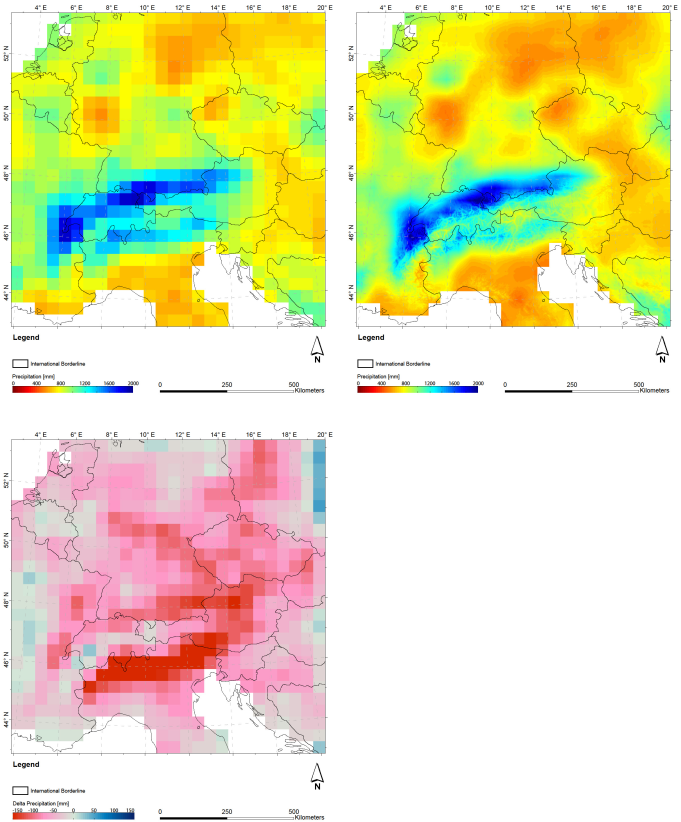

Fig. 14. Mean annual precipitation [mm] (01.01.1996–31.12.1999) of MM5 simulations, fully coupled with the NOAH-LSM for providing the lower boundary conditions at a spatial resolution of 45 km (upper left) and fully coupled with PROMET at a spatial resolution of 1 km (upper right). Difference between fully coupled PROMET and fully coupled NOAH-LSM simulation (lower left).

HESSD
8, 7091–7136, 2011

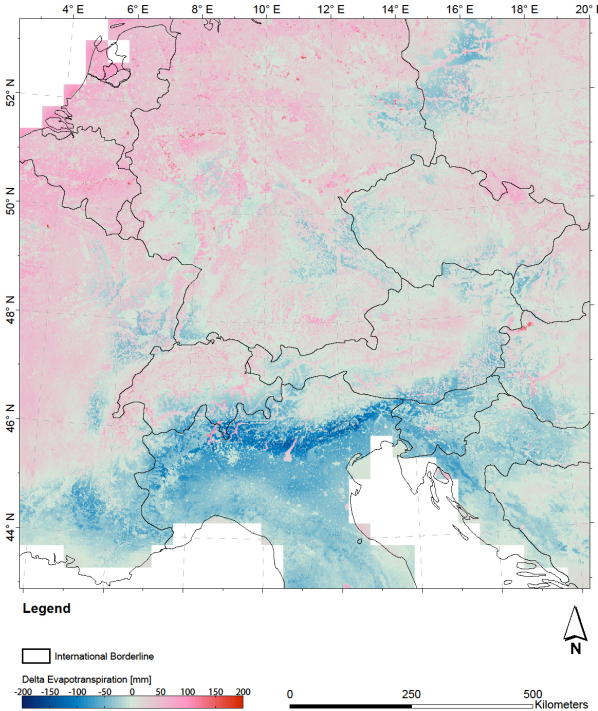

Fig. 15. Subtraction image of bilaterally and unilaterally coupled PROMET simulation of mean annual evapotranspiration (1 × 1 km).

HESSD
8, 7091–7136, 2011

Inter-comparison of two land-surface schemes

F. Zabel et al.

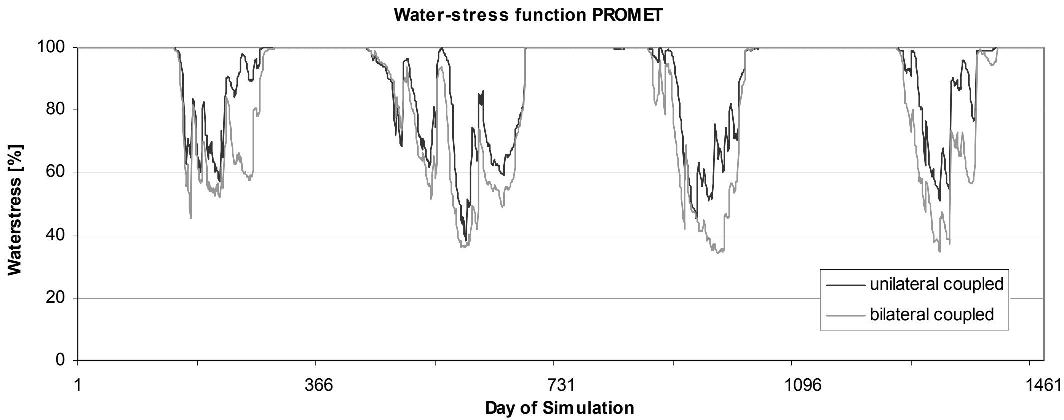

Fig. 16. Comparison of unilaterally and bilaterally coupled water stress function in PROMET for the vegetated PROMET pixels of the Milan pixels.